



This document is the accepted manuscript version of a published work that appeared in final form in *International Journal of Greenhouse Gas Control*, © Elsevier, after peer review and technical editing by the publisher. To access the final edited and published work, see [http://dx.doi.org/10.1016/s1750-5836\(07\)00107-7](http://dx.doi.org/10.1016/s1750-5836(07)00107-7)

(Article begins on next page)

# Novel oxygen-carrier materials for chemical-looping combustion and chemical-looping reforming; $\text{La}_x\text{Sr}_{1-x}\text{Fe}_y\text{Co}_{1-y}\text{O}_{3-\delta}$ perovskites and mixed-metal oxides of $\text{NiO}$ , $\text{Fe}_2\text{O}_3$ and $\text{Mn}_3\text{O}_4$

Magnus Rydén\*, Anders Lyngfelt, Tobias Mattisson  
Department of Energy and Environment  
Chalmers University of Technology  
SE-412 96, Göteborg, Sweden

De Chen, Anders Holmen  
Department of Chemical Engineering  
Norwegian University of Science and Technology  
N-9491, Trondheim, Norway

Erlend Bjørgum  
SINTEF Materials and Chemistry  
N-9491, Trondheim, Norway

## Abstract

Solid oxygen-carrier materials for chemical-looping applications have been examined by reduction with  $\text{CH}_4$  and oxidation with air in a fixed-bed quartz reactor at  $900^\circ\text{C}$ . Four perovskite materials, three metal-oxide materials and four metal-oxide mixtures have been studied. It was found that  $\text{La}_x\text{Sr}_{1-x}\text{FeO}_{3-\delta}$  perovskites provided very high selectivity towards  $\text{CO}/\text{H}_2$  and should be well suited for chemical-looping reforming. Substituting La for Sr was found to increase the oxygen capacity of these materials, but reduced the selectivity towards  $\text{CO}/\text{H}_2$  and the reactivity with  $\text{CH}_4$ .  $\text{La}_{0.5}\text{Sr}_{0.5}\text{Fe}_{0.5}\text{Co}_{0.5}\text{O}_{3-\delta}$  was found to be feasible for chemical-looping combustion applications.  $\text{NiO}/\text{MgAl}_2\text{O}_4$  propagated formation of solid carbon, likely due to the catalytic properties of metallic Ni.  $\text{Fe}_2\text{O}_3/\text{MgAl}_2\text{O}_4$  had properties that made it interesting both for chemical-looping combustion and chemical-looping reforming. Adding 1% NiO particles to a bed of  $\text{Fe}_2\text{O}_3$ -particles increased both reactivity with  $\text{CH}_4$  and selectivity towards  $\text{CO}/\text{H}_2$  for reforming applications.  $\text{Mn}_3\text{O}_4/\text{Mg-ZrO}_2$  was found to be suitable for chemical-looping combustion applications, but it could not be verified that adding NiO produced any positive effects.

*Keywords:* Chemical-Looping Combustion; Chemical-Looping Reforming; Partial Oxidation; Perovskites; Hydrogen; Synthesis Gas.

## 1. Introduction

In later years, concerns that emissions of  $\text{CO}_2$  from combustion of fossil fuels may lead to changes in the climate of the earth have been growing steadily. A majority of the scientific community now concludes that global  $\text{CO}_2$  emissions would need to be reduced greatly in the future. This is a huge task, because whether we like it or not our current dependence on fossil fuels can hardly be overestimated.

---

\*Corresponding author: Tel. (+46) 31 7721457, Email: [magnus.ryden@chalmers.se](mailto:magnus.ryden@chalmers.se)  
*International Journal of Greenhouse Gas Control* 2008; 2: 21-36.

One way to reduce CO<sub>2</sub> emissions that is receiving increasing interest is CO<sub>2</sub> sequestration, which is the capture of CO<sub>2</sub> in an emission source and storing it where it is prevented from reaching the atmosphere. This could involve for example CO<sub>2</sub> capture in flue gases from combustion processes, and CO<sub>2</sub> storage in geological formations such as depleted oil and gas fields or deep saline aquifers. Carbon sequestration has potential to greatly reduce CO<sub>2</sub> emissions from large point sources such as power plants and industries.

In contrast, CO<sub>2</sub> capture applications for small mobile emission sources such as cars, trucks and airplanes seem implausible. This is noteworthy since the transportation sector alone is responsible for about one quarter of the global CO<sub>2</sub> emissions, and this share is increasing. Most likely, CO<sub>2</sub> capture would also be complicated and expensive for small scale applications due to unfavourable economics of scale.

There are ways to address this dilemma though. It is well established that fossil fuels can be converted into H<sub>2</sub> via various reforming processes. So if CO<sub>2</sub> is captured within the reforming process, produced H<sub>2</sub> could be used as a CO<sub>2</sub>-free fuel for vehicles, as well as for other applications. H<sub>2</sub> is a versatile energy carrier that can be burnt in combustion engines or gas turbines. It is also the ideal fuel for most types of fuel cells, which are applications that promises much higher efficiency than conventional engines. Fuel cells are well suited for small and medium scale power generation. H<sub>2</sub> can also be mixed with other gaseous fuels.

The chemical-looping concept involves oxidation of a fuel using oxygen from a solid oxygen carrier instead of oxygen from air. This way the products are not diluted with N<sub>2</sub>. The chemical-looping concept is interesting both for CO<sub>2</sub> capture applications in combustion processes, and for H<sub>2</sub> generation through reforming processes. One key issue with the chemical-looping concept that needs to be studied further is the oxidation and reduction behaviour of potential oxygen-carrier materials. In this paper, four different La<sub>x</sub>Sr<sub>1-x</sub>Fe<sub>y</sub>Co<sub>1-y</sub>O<sub>3-δ</sub> perovskites are examined by reduction with CH<sub>4</sub> and oxidation with air. Three oxygen-carriers based on NiO, Fe<sub>2</sub>O<sub>3</sub> and Mn<sub>3</sub>O<sub>4</sub> have also been examined, as well as four oxide mixtures of Fe<sub>2</sub>O<sub>3</sub> or Mn<sub>3</sub>O<sub>4</sub> with some added NiO.

The layout of the paper is as follows. In section 2, the concepts of chemical-looping combustion and chemical-looping reforming are explained, as well as the basic characteristics of La<sub>x</sub>Sr<sub>1-x</sub>Fe<sub>y</sub>Co<sub>1-y</sub>O<sub>3-δ</sub> perovskites. In section 3, the experimental procedures are described. In section 4, the results of the experiments are presented. In section 5, the results and their implications are discussed.

## **2. Technical Background**

### **2.1 Chemical-Looping Combustion**

Chemical-looping combustion is an innovative combustion technology that can be used for CO<sub>2</sub> capture in power generating processes. Two separate reactors are used, one for air and one for fuel. A solid oxygen carrier performs the task of transporting oxygen between the reactors. Hence direct contact between fuel and air is avoided and the combustion products are not diluted with N<sub>2</sub>, see Figure 1.

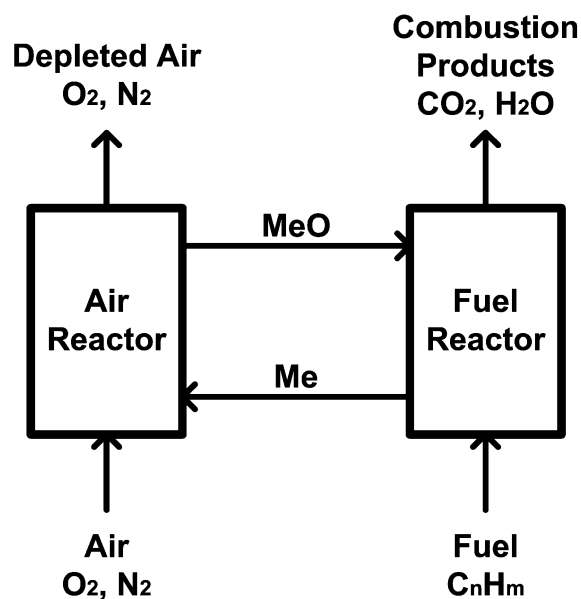


Figure 1. Schematic description of chemical-looping combustion.

Typically, the abbreviation MeO is used to describe the oxygen carrier in its oxidized form, while Me is used for the reduced form. This is because many potential oxygen-carrier materials are metal oxides, for example NiO, Fe<sub>2</sub>O<sub>3</sub>, Mn<sub>3</sub>O<sub>4</sub> and CuO.

The oxygen carrier circulates between the reactors. In the fuel reactor, it is reduced by the fuel, which in turn is oxidized to CO<sub>2</sub> and H<sub>2</sub>O according to reaction (1). In the air reactor, it is oxidized to its initial state with O<sub>2</sub> from the combustion air according to reaction (2).

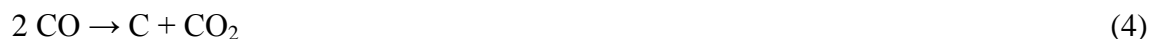


The amount of energy released or required in each reactor vessel depends on the nature of the oxygen carrier and the fuel. Reaction (2) is always strongly exothermic. For most oxygen-carrier materials, reaction (1) is endothermic if the fuel is a hydrocarbon. If CO or H<sub>2</sub> is used as fuel, reaction (1) is slightly exothermic. If reaction (1) is endothermic the flow of solid oxygen carrier can be used to transport sensible heat from the air reactor to the fuel reactor. The net energy released in the reactor system is the same as for ordinary combustion. This is apparent since combining reaction (1) and reaction (2) yields reaction (3), which is complete combustion of the fuel with O<sub>2</sub>.



Compared with conventional combustion, chemical-looping combustion has several potential benefits. The exhaust gas from the air reactor is harmless, consisting mainly of N<sub>2</sub> and possibly some O<sub>2</sub>. There should be no thermal formation of NO<sub>x</sub> since regeneration of the oxygen carrier takes place without flame and at moderate temperatures, from about 800°C and up. The gas from the fuel reactor consists of CO<sub>2</sub> and H<sub>2</sub>O, so cooling in a condenser is all that is needed to obtain almost pure CO<sub>2</sub>. This is a major advantage with chemical-looping combustion. About three quarters of the energy required for CO<sub>2</sub> capture and storage with conventional methods, such as amine scrubbing of flue gases, is associated with the separation of CO<sub>2</sub> and N<sub>2</sub>. With chemical-looping combustion this can be avoided completely since fuel and air are not mixed, and therefore no gas separation is needed.

Possible side reactions include formation of solid carbon in the fuel reactor. This is unwanted since solid carbon could follow the oxygen-carrier circulation to the air reactor and burn there, which would reduce the degree of CO<sub>2</sub> capture. Solid carbon could be formed either through the Boudouard reaction, reaction (4), or through hydrocarbon decomposition, reaction (5). Formation of solid carbon is well documented from various chemical processes, and it is known that reactions (4-5) can be catalysed by metallic surfaces or carbon.



In later years when the interest for carbon sequestration has increased chemical-looping combustion has become an active research issue. The research has focused on experimental and theoretical investigations of possible oxygen-carriers and on process studies of how chemical-looping combustion could be used for power generation. A feasible oxygen-carrier material for chemical-looping combustion should:

- Have high reactivity with fuel and oxygen.
- Be thermodynamically capable to convert a large share of the fuel to CO<sub>2</sub> and H<sub>2</sub>O.
- Have low tendency towards fragmentation, attrition, agglomeration and other kinds of mechanical or thermal degeneration.
- Not promote extensive formation of solid carbon in the fuel reactor.
- Be cheap and preferably environmentally sound.

At present, metal oxides such as NiO, Fe<sub>2</sub>O<sub>3</sub>, Mn<sub>3</sub>O<sub>4</sub> and CuO supported on inert carrier material such as Al<sub>2</sub>O<sub>3</sub>, ZrO<sub>2</sub> or MgAl<sub>2</sub>O<sub>4</sub> seem like the most likely candidates to meet those criteria. An overview of the research dealing with these kinds of oxygen-carriers can be found in the works of Cho (2005a), Johansson, M. (2005) and Adánez et al. (2003). Information about other potential oxygen-carrier materials can be found in the work of Jerndal et al. (2006), which includes a theoretical examination of 27 different oxide systems. Carbon formation on oxygen-carrier particles for chemical-looping combustion has been specifically examined by Cho et al. (2005b).

In practice, a chemical-looping combustion process could be designed in different ways, but circulating fluidized beds with oxygen-carrier particles used as bed material are likely to have an advantage over other alternatives since this design is straightforward, provides good contact between gas and solids and allows a smooth flow of oxygen carrier between the reactors. Continuous chemical-looping combustion in circulating fluidized beds has been demonstrated by Lyngfelt et al. (2004), Ryu et al. (2004), Johansson, E. et al. (2006a, 2006b) Abad et al. (2006, 2007) and Adanez et al. (2006).

An overview of various subjects regarding chemical-looping combustion, such as design of experimental reactors, power production with CO<sub>2</sub> capture and more about oxygen-carrier materials can be found in the doctoral theses by Brandvoll (2005), Johansson, E. (2005), Wolf (2004), Kronberger (2005) and Naqvi (2006).

## 2.2 Chemical-Looping Reforming

Chemical-looping reforming, as described in this paper, was proposed in 2001 by Mattisson and Lyngfelt (2001). It utilizes the same basic principles as chemical-looping combustion. The difference is that the products wanted are not heat but synthesis gas, a mix of H<sub>2</sub> and CO. Therefore the air to fuel ratio is kept low to prevent the fuel from becoming fully oxidized to CO<sub>2</sub> and H<sub>2</sub>O. Chemical-looping reforming in its most basic form could be

described as a process for partial oxidation of hydrocarbon fuels where a solid oxygen carrier is used as a source of undiluted oxygen. This is favourable since it would eliminate the need for expensive and power demanding air separation. The basic principles of chemical-looping reforming are illustrated in Figure 2.

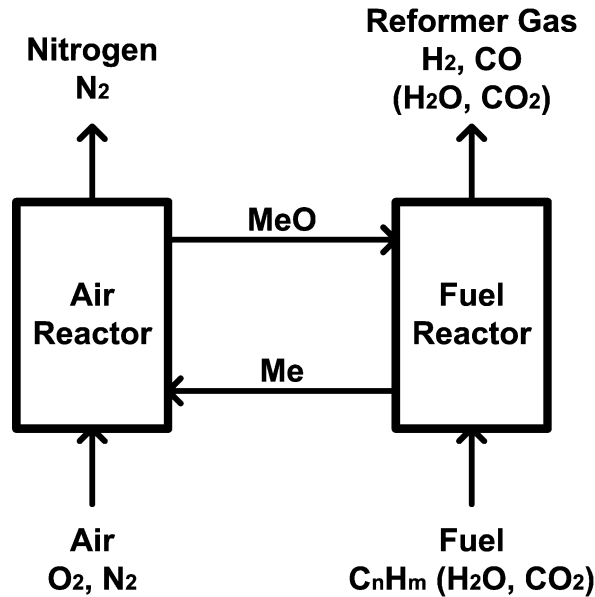
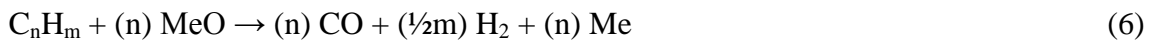


Figure 2. Schematic description of chemical-looping reforming.

In the air reactor, reaction (2) will occur, just as in chemical-looping combustion. In the fuel reactor, some fuel may become completely oxidized to  $\text{CO}_2$  and  $\text{H}_2\text{O}$  via reaction (1), but a large share should react according to reaction (6), partial oxidation using oxygen from the oxygen carrier.



If synthesis gas particularly rich with  $\text{H}_2$  or  $\text{CO}$  is wanted, steam or  $\text{CO}_2$  could be added to the fuel to enhance the relative importance of steam reforming, reaction (7), or  $\text{CO}_2$  reforming, reaction (8), respectively. Adding  $\text{H}_2\text{O}$  or  $\text{CO}_2$  to the fuel would likely also suppress formation of solid carbon.



The overall reaction energy of the reactor system varies as the relative importance between reactions (1-2) and reactions (6-8) is altered. When the fuel and oxygen carrier reacts according to reaction (1) and reaction (2), heat corresponding to the lower heating value of the fuel is released. When the fuel reacts according to reaction (6) and reaction (2), minor amounts of heat is released corresponding to the reaction energy for partial oxidation of the fuel. Reaction (7-8) are strongly endothermic and do not provide any reduced oxygen carrier to be reoxidized with the exothermic reaction (2). Hence steam reforming and  $\text{CO}_2$  reforming can not be allowed to dominate the process since this would make the reactor system endothermic, and external heating of the reactors at relevant temperatures would likely be unfavourable from a technical point of view.

The outlet from the fuel reactor consists of  $H_2$ ,  $H_2O$ ,  $CO$  and  $CO_2$ , and could be used as feedstock for chemical processes or for production of  $H_2$ , just as synthesis gas from other reforming processes. Due to reaction kinetics and thermodynamics it is possible that there will be some unreformed  $CH_4$  in the reformer gas if the reactor temperature is not sufficiently high. If thermodynamic equilibrium is assumed, a fuel reactor temperature in the order of  $800^\circ C$  should be sufficient to achieve 99% conversion of  $CH_4$  at atmospheric pressure. At elevated pressure, temperatures over  $1000^\circ C$  may be needed.

Oxygen-carrier materials for chemical-looping reforming would need to have about the same properties as those for chemical-looping combustion. The main difference is that they must be capable to convert the fuel to  $CO$  and  $H_2$  when the air to fuel ratio is reduced, rather than produce  $CO_2$ ,  $H_2O$  and unreformed fuel. Furthermore, the oxygen carrier should be resistant towards carbon formation since decomposition of the fuel, reaction (5), is believed to be a bigger issue for chemical-looping reforming than for chemical-looping combustion.

Oxygen carriers specifically for chemical-looping reforming have been examined by Zafar et al. (2005), who performed tests in a fluidized-bed reactor with oxygen-carrier particles as fluidizing agent, and by Mattisson et al. (2004). These two studies indicate high reaction rate and good selectivity towards  $H_2$  and  $CO$  for oxygen carriers with  $NiO$  as active phase, while oxygen carriers based on  $Fe_2O_3$ ,  $Mn_3O_4$  and  $CuO$  suffered from poor selectivity and produced mostly  $CO_2$ ,  $H_2O$  and unreformed  $CH_4$ . Continuously operating chemical-looping reforming in a circulating-fluidized bed reactor has been demonstrated by Rydén et al. (2006a), who found that chemical-looping reforming of natural gas with an oxygen-carrier consisting of 60 mass%  $NiO$  supported on  $MgAl_2O_4$  was feasible, but that carbon formation could be an obstacle unless the fuel was mixed with some steam. An overview of various subjects regarding chemical-looping reforming can be found in the licentiate thesis by Rydén (2006b).

In later years, other process concepts sharing attributes with chemical-looping reforming have also been proposed. Stobbe et al. (1999) have suggested a process involving oxidation and reduction of manganese oxide. Fathi et al. (2000), Gavalas et al. (2000) and Jalibert et al. (2001) have suggested and examined partial oxidation of  $CH_4$  by oxidation and reduction of  $CeO_2$  promoted with noble-metal catalysts. Other studies have examined  $La_xSr_{1-x}Fe_yCo_{1-y}O_{3-\delta}$  perovskites for the same purpose, see section 2.4 below.

### 2.3 Mixed Metal Oxides as Oxygen Carrier

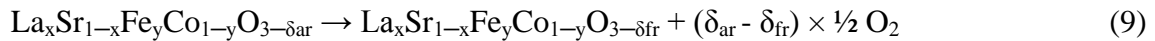
From the early years of chemical-looping combustion research it is well established that  $NiO$  have high reactivity with  $CH_4$  and other hydrocarbons. Metallic surfaces catalyze decomposition of  $CH_4$ , so once some  $NiO$  is reduced to  $Ni$  the conversion of  $CH_4$  to other components is rapid. Materials like  $Fe_2O_3$  and  $Mn_3O_4$  are reduced to new oxide phases rather than to metals. Hence it is not surprising that these materials generally have shown less reactivity with  $CH_4$ . On the other hand,  $Fe_2O_3$  and  $Mn_3O_4$  have proven to be highly reactive with  $CO$  and  $H_2$ . Compared to  $NiO$ ,  $Fe_2O_3$  and  $Mn_3O_4$  also have the advantage of being cheaper and more environmentally benign. Hence combining different oxygen-carrier materials may create positive synergy effects. Small amounts of metallic  $Ni$  could be sufficient to catalyze decomposition of  $CH_4$  into more reactive components such as  $CO$  and  $H_2$ , whereas the bulk of the oxygen could be provided with another material. The option to use mixtures of  $NiO$  and  $Fe_2O_3$  as oxygen-carrier for chemical-looping combustion have been demonstrated by Johansson, M. et al. (2006a), who found that small amounts of  $NiO$  increased the reaction rate of the  $Fe$ -based oxygen carrier considerably. Mixed-metal oxides could be a way to combine the reactivity of  $NiO$  and the viability of  $Fe_2O_3$  and  $Mn_3O_4$ , so there are good reasons to study this concept further.

## 2.4 $\text{La}_x\text{Sr}_{1-x}\text{Fe}_y\text{Co}_{1-y}\text{O}_{3-\delta}$ Perovskites

$\text{La}_x\text{Sr}_{1-x}\text{Fe}_y\text{Co}_{1-y}\text{O}_{3-\delta}$  are ceramic materials of perovskite structure. This structure has a unit cell with the general formula  $\text{ABO}_3$ , where A is a large cation and B is a smaller cation. Typically A is an alkali metal, an alkaline earth metal or a rare earth metal while B is a transition metal. The ideal perovskite structure can be described as a  $\text{BO}_6$  octahedral, with A occupying the centre. Sometimes there are flaws in the structure. Most commonly, such flaws arise from oxygen deficiency. Hence the perovskite structure is often written  $\text{ABO}_{3-\delta}$ , where  $\delta$  expresses the amount of oxygen deficiency. In a  $\text{La}_x\text{Sr}_{1-x}\text{Fe}_y\text{Co}_{1-y}\text{O}_{3-\delta}$  perovskite structure A is La or Sr, while B is Fe or Co.

$\text{La}_x\text{Sr}_{1-x}\text{Fe}_y\text{Co}_{1-y}\text{O}_{3-\delta}$  perovskites are interesting for many applications, notably as oxygen permeable membranes, for manufacturing of various high temperature electrochemical devices, and as catalyst for oxidation reactions. They have very high thermal stability and decent mechanical properties. The doctoral theses by Fossdal (2003) and Lea Lein (2005) are good sources for general information about this kind of materials.

The  $\delta$ -factor in  $\text{La}_x\text{Sr}_{1-x}\text{Fe}_y\text{Co}_{1-y}\text{O}_{3-\delta}$  perovskites can be reduced or increased by altering factors in the surroundings such as temperature or  $\text{O}_2$  partial pressure. This ability makes  $\text{La}_x\text{Sr}_{1-x}\text{Fe}_y\text{Co}_{1-y}\text{O}_{3-\delta}$  perovskites potentially useful for chemical-looping applications. The environment in a chemical-looping air reactor is oxidative. Hence  $\delta_{\text{ar}}$  will be small. In the fuel reactor, the environment is reductive, so  $\delta_{\text{fr}}$  will be large. The amount of  $\text{O}_2$  available for oxidation of fuel can be written as  $(\delta_{\text{ar}} - \delta_{\text{fr}})$ , see expression (9).



Blom et al. (2005) have proposed and examined the possibility to use  $\text{La}_x\text{Sr}_{1-x}\text{Fe}_y\text{Co}_{1-y}\text{O}_{3-\delta}$  perovskites as oxygen carriers for chemical-looping combustion. Shen et al. (2002, 2004), Zeng et al. (2003), Li et al. (2005) and Bjørgum (2005) has studied the possibility to generate synthesis gas by cyclic oxidation and reduction of perovskites such as  $\text{La}_x\text{Sr}_{1-x}\text{Fe}_y\text{Co}_{1-y}\text{O}_{3-\delta}$ , in similar fashion as is done in chemical-looping reforming. The conclusions drawn in these studies have generally been encouraging. Hence there are good reasons to examine this potential application of  $\text{La}_x\text{Sr}_{1-x}\text{Fe}_y\text{Co}_{1-y}\text{O}_{3-\delta}$  perovskites further.

## 2.5 The Aim of This Study

The aim of this study is to examine oxygen-carrier materials for chemical-looping applications, particularly for chemical-looping reforming. Novel options such as  $\text{La}_x\text{Sr}_{1-x}\text{Fe}_y\text{Co}_{1-y}\text{O}_{3-\delta}$  perovskites and mixed-metal oxides have been compared to more traditional materials. Factors that have been studied are reactivity with  $\text{CH}_4$ , product composition of produced gas, oxygen-carrier capacity expressed as mass% of the sample and tendency to propagate formation of solid carbon.

## 3. Experimental

### 3.1 Preparation of Oxygen-Carrier Materials

$\text{La}_x\text{Sr}_{1-x}\text{Fe}_y\text{Co}_{1-y}\text{O}_{3-\delta}$  perovskites were synthesized with the glycine-nitrate combustion method and spray drying. The obtained materials were ball-milled in ethanol, calcined and sieved to particles with a suitable size. Details about the manufacturing process and material characterisation such as x-ray powder diffraction (XRD), temperature programmed reduction

(TPR) and temperature programmed surface reaction (TPSR) can be found in the work of Bjørgum (2005). Data for produced perovskite materials can be found in Table 1.

Sample	Material	Particle Size ( $\mu\text{m}$ )	Calcination (T/time)
1	$\text{La}_{0.5}\text{Sr}_{0.5}\text{Fe}_{0.5}\text{Co}_{0.5}\text{O}_{3-\delta}$	150-250	900°C/24 hours
2	$\text{LaFeO}_{3-\delta}$	150-250	900°C/10 hours
3	$\text{La}_{0.8}\text{Sr}_{0.2}\text{FeO}_{3-\delta}$	150-250	900°C/10 hours
4	$\text{La}_{0.5}\text{Sr}_{0.5}\text{FeO}_{3-\delta}$	150-250	900°C/10 hours

*Table 1. Produced perovskite materials*

Metal-oxide particles were produced by freeze granulation, dried in a freeze-drier, sintered and sieved to a suitable size range. Details about the manufacturing process can be found in the work of Cho (2005) and Johansson, M. (2005). Data for produced metal-oxide materials can be found in Table 2.

Sample	Material	Designation	Particle Size ( $\mu\text{m}$ )	Sintering (T/time)
5	60% NiO on $\text{MgAl}_2\text{O}_4$	Ni100	90-150	1400°C/6 hours
6	40% $\text{Fe}_2\text{O}_3$ on $\text{MgAl}_2\text{O}_4$	Fe100	90-125	1100°C/6 hours
7	40% $\text{Mn}_3\text{O}_4$ on $\text{Mg-ZrO}_2$	Mn100	90-125	1150°C/6 hours

*Table 2. Produced metal-oxide materials*

In addition to the pure samples, a few oxide mixtures were also examined. These were prepared simply by mixing particles of the oxygen-carriers in Table 2 in various proportions. Data for the mixed-oxide samples can be found in Table 3. All percentages in Table (1-3) are mass%.

Sample	Designation	Composition
8	Fe99Ni1	99% Fe100 and 1% Ni100
9	Fe90Ni10	90% Fe100 and 10% Ni100
10	Mn97Ni3	97% Mn100 and 3% Ni100
11	Mn90Ni10	90% Mn100 and 10% Ni100

*Table 3. Examined mixed-oxide materials*

### 3.2 Experimental Setup

The experiments were carried out in a quartz reactor with a diameter of 15 mm and a height of 350 mm. The reactor was located inside a vertical electrically heated furnace. The temperature of the furnace was controlled with a thermoelement located inside the reactor. In the centre of the reactor there was a porous plate, on which a sample of particles could be located. The top of the reactor was connected to a gas feeding system, capable of handling  $\text{CH}_4$ , air, Ar,  $\text{CO}_2$  and calibration gas. The bottom of the reactor was connected to an outlet pipe. The products were analyzed with a mass spectrometer. Between the reactor outlet and the mass spectrometer, the pipe was heated with an electric heating strip to prevent condensation of  $\text{H}_2\text{O}$  prior to analysis.

It shall be noticed that fixed-bed reactors are not the most common way to do chemical-looping experiments and has some potential drawbacks. Different reactions may take place at the same time at different locations in the bed. It is also difficult to control the temperature in

the bed when there are endothermic or exothermic reactions occurring. The main reason for using a fixed-bed reactor was that it is possible to do such experiment using only a small amount of active material. The commonly used alternative for such experiments, Thermo Gravimetric Analysis (TGA), does not provide any information about the selectivity towards H<sub>2</sub> and CO, which is necessary when examining materials for chemical-looping reforming applications. Another option would have been to use a fluidized-bed reactor, but this would have required much larger material samples. Additionally, the perovskites were not manufactured with fluidized-bed reactors in mind. The implications of the reactor choice are discussed further in section 5 below.

### 3.3 Experimental Procedure

A sample of 1.00 gram of the chosen material was added to the reactor. Then the reactor system was assembled and the mass spectrometer calibrated. Then the reactor was heated to 900°C. During this time Ar was used to provide the necessary gas flow through the reactor and the mass spectrometer. When 900°C was reached, the sample was reduced with CH<sub>4</sub>. Ar was used as carrier gas so that the total gas flow into the reactor was 60 ml/min. This was done to provide reasonable response time for the lower CH<sub>4</sub> flows. For most experiments the reduction period was 10 minutes. For samples of Mn<sub>3</sub>O<sub>4</sub>, a shorter reduction period was used, due to the relatively low oxygen content of this material. For samples reduced with high CH<sub>4</sub> flows the reduction period was also shortened somewhat, since high CH<sub>4</sub> flows resulted in more rapid reduction of the samples. In many published experiments where oxygen-carrier materials for chemical-looping applications are tested the fuel is diluted with steam rather than Ar, in order to prevent formation of solid carbon. This was not done here since one of the aims was to study if and when carbon formation occurs on different materials.

Following the reduction of the sample was an inert period of about one minute, during which Ar was fed to the reactor. Then the sample was reoxidized with 60 ml/min air. The duration of the oxidation period depended on the degree of reduction of the sample, and the degree of carbon formation. The reoxidation was aborted when the measured signals of N<sub>2</sub> and O<sub>2</sub> in the reactor outlet were stable. Then there was another short inert period, lasting about 30 seconds. This was necessary to prevent mixing of CH<sub>4</sub> and air prior to the reactor. After this short period of time a new reduction cycle was initiated.

The procedure described above was repeated for 10 cycles for each perovskite, in which the CH<sub>4</sub> flow was varied between 9 ml/min and 33 ml/min. This corresponds to 56-206 kg solids for each MW of thermal power added with the fuel. For metal oxide samples, 5 cycles with CH<sub>4</sub> flows between 15 ml/min and 27 ml/min was used. The complete test matrix can be found in Table 4.

Sample	Material/Designation	Cycle number and CH <sub>4</sub> flow (ml/min, room temperature)									
		1	2	3	4	5	6	7	8	9	10
1	La <sub>0.5</sub> Sr <sub>0.5</sub> Fe <sub>0.5</sub> Co <sub>0.5</sub> O <sub>3-δ</sub>	9	9	15	15	21	21	27	27	33	9
2	LaFeO <sub>3-δ</sub>	9	9	15	15	21	21	27	27	33	9
3	La <sub>0.8</sub> Sr <sub>0.2</sub> FeO <sub>3-δ</sub>	9	9	15	15	21	21	27	27	33	9
4	La <sub>0.5</sub> Sr <sub>0.5</sub> FeO <sub>3-δ</sub>	9	9	15	15	21	21	27	27	33	9
5	Ni100	15	15	15	27	27					
6	Fe100	15	15	15	27	27					
7	Mn100	15	15	15	27	27					
8	Fe99Ni1	15	15	15	27	27					
9	Fe90Ni10	15	15	15	27	27					
10	Mn97Ni3	15	15	15	27	27					
11	Mn90Ni10	15	15	15	27	27					

Table 4. Test matrix describing the reduction cycles for each tested material.

### 3.4 Evaluation of Measured Data

The most interesting data is the outlet concentration of CH<sub>4</sub>, CO<sub>2</sub>, H<sub>2</sub>, H<sub>2</sub>O and CO from the reactor during reduction with CH<sub>4</sub>. The concentration of O<sub>2</sub> and N<sub>2</sub> was also measured but these components were not present during reduction. The composition of the outlet gas during reoxidation is of less interest. In previous studies of oxygen carrier material for chemical-looping combustion it has been found that reoxidation of an oxygen-carrier material is often much faster and less problematic than reduction. This was true for the experiments presented here as well, both for metal-oxide materials and perovskite materials. At no occasion did O<sub>2</sub> pass through the reactor system until the sample was regenerated. Hence the performed experiments are unable to provide any quantitative information about the kinetics of the reoxidation reaction, other than that it was faster than the reduction reaction. The gas concentrations during oxidation could have been used to quantify the amount of carbon formation accumulated on the sample, but measured data from the reduction period also provided this information, and as a function of time.

The method of choice for gas analysis was mass spectroscopy. Compared to the alternatives, mass spectroscopy has the advantage of being capable to measure all relevant gas components continuously, including H<sub>2</sub> and H<sub>2</sub>O. There are some minor drawbacks though. Firstly, it is complicated to distinguish between N<sub>2</sub> and CO since these two gases have the same molecular mass. But N<sub>2</sub> was only present during reoxidation of the perovskites, so this should not have been a problem. Secondly, there are also minor interferences due to molecules briefly converted into ions during analysis. This has been accounted for in the way that is proposed in the documentation of the mass spectrometer.

The mass spectrometer was calibrated each day by mixing relevant proportions of Ar, CH<sub>4</sub>, CO<sub>2</sub>, air and calibration gas consisting of mainly H<sub>2</sub> and CO. The experimental setup lacked the option to feed steam directly into the reactor, which made calibration of H<sub>2</sub>O tricky. According to the instrument documentation H<sub>2</sub>O should have approximately the same calibration data as O<sub>2</sub> and N<sub>2</sub>. This assumption could be verified by comparing the H<sub>2</sub>O and CO<sub>2</sub> signals in the beginning of each reduction period, where for most experiments complete oxidation of CH<sub>4</sub> to H<sub>2</sub>O and CO<sub>2</sub> should occur, and the H<sub>2</sub>O concentration should be twice as high as the CO<sub>2</sub> concentration. With this information, it was possible to relate the signal for H<sub>2</sub>O to the signal for CO<sub>2</sub> and calibrate H<sub>2</sub>O with reasonable accuracy.

The mass spectrometer provided the actual gas concentrations including inert Ar, which was present as carrier gas. To make it easier to compare experiments with different flows of CH<sub>4</sub> and Ar, the gas composition was converted to a product composition that excluded Ar, see expression (10). Here  $x$  is the calculated product composition and  $y$  is the measured concentration of each component.

$$x_i = y_i / [ y_{CO_2} + y_{CO} + y_{CH_4} + y_{H_2O} + y_{H_2} ] \quad (10)$$

Each measuring cycle with the mass spectrometer took several seconds to complete, and at least one second for each measured component. Hence there could be several seconds between measured concentrations of two gas components, while the software packaged and delivered them as one single measuring point. When there were large concentration gradients this had implications. Notably, the proportion between CO<sub>2</sub> and H<sub>2</sub>O sometimes looked strange in the beginning of each reduction cycle, where the concentration of the various gas components changes rapidly. The higher the CH<sub>4</sub> flow, the larger became this effect. Hence the focus in this paper is on the results obtained with CH<sub>4</sub> flows of 15 ml/min or lower.

Since all relevant gas components were measured during reduction and the hydrogen to carbon ratio for CH<sub>4</sub>,  $(H/C)_{CH_4}$ , is known, formation of solid carbon on the particles,  $c$ , could be calculated with a species balance, see expression (11).

$$(H/C)_{CH_4} = 4 = [ 2 \times x_{H_2O} + 2 \times x_{H_2} + 4 \times x_{CH_4} ] / [ x_{CO_2} + x_{CO} + x_{CH_4} + c ] \quad (11)$$

The carbon formation could then be expressed as a percentage of the total amount of carbon added with the CH<sub>4</sub>,  $c/c_{tot}$ , see expression (12).

$$c/c_{tot} = c / [ x_{CO_2} + x_{CO} + x_{CH_4} + c ] \quad (12)$$

Under most circumstances the calculated values for  $c/c_{tot}$  were found to fluctuate around zero, ranging from about -4% to +4%. At 900°C decomposition of CH<sub>4</sub> to carbon is auto-catalytic, so these kind of small fluctuations do not seem likely to occur in reality. Hence the behaviour is believed to have been an effect of the way the used software presented measured data, so for the evaluation  $c/c_{tot}$  was set to zero until the calculated value reached 4%. Within this period, the species composition was balanced by adjusting  $x_{H_2O}$ .

The oxygen content  $R_0$  is an important property of oxygen carriers for chemical-looping applications. It is defined in expression (13), where  $m_{ox}$  is the mass of the completely oxidized sample and  $m_{red}$  is the mass of the completely reduced sample.

$$R_0 = [ m_{ox} - m_{red} ] / m_{ox} \quad (13)$$

$R_0$  describes how much oxygen expressed in mass% of the oxidized sample that theoretically could be released during operation. For particles of highly reactive metal oxides such as NiO, values close to  $R_0$  could be obtained. For La<sub>x</sub>Sr<sub>1-x</sub>Fe<sub>y</sub>Co<sub>1-y</sub>O<sub>3-δ</sub> perovskites the picture is somewhat different. In theory these materials have  $R_0$  values in the order of 20% due to their large oxygen content. But only a limited amount of this oxygen could probably be released during operation. For a stable perovskite structure, the kinetics of oxygen removal should slow down greatly when a certain amount of oxygen has been removed and eventually stop. Less stable perovskites structures may undergo irreversible changes or break up into metal oxides when large amounts of oxygen is removed, see for example Blom et al. (2005).

The mass based conversion of an oxygen carrier  $\omega$  is defined in expression (14), where  $m$  is the actual weight of the sample.

$$\omega = m / m_{ox} = 1 + R_0 \times [ X - 1 ] \quad (14)$$

In this paper, the amount of oxygen released from a sample is most often expressed in mass% of the oxidized sample  $\Delta\omega$  which is defined in expression (15).

$$\Delta\omega = 1 - \omega = [ m_{ox} - m ] / m_{ox} \quad (15)$$

Since no oxygen was added to the reactor during the reduction period it is possible to calculate the amount of oxygen that was released from the sample as a function of time by using measured values for oxygen to carbon ratio for the product gas,  $(O/C)_{products}$ , see expressions (16-17), where  $M_O$  is the molar mass of oxygen,  $F_{CH_4}$  is the molar flow of CH<sub>4</sub> added to the reactor and  $\Delta t$  is a period of time.

$$(O/C)_{products} = [ 2 \times x_{CO_2} + x_{H_2O} + x_{CO} ] / [ x_{CO_2} + x_{CO} + x_{CH_4} + c ] \quad (16)$$

$$d\omega/dt = [ (O/C)_{products, average for \Delta t} \times (F_{CH_4} \times \Delta t) \times (M_O / m_{ox}) ] / \Delta t \quad (17)$$

The amount of oxygen released under a particular amount of time is obtained by integrating expression (17), see expression (18).

$$\Delta\omega = [ (O/C)_{products, average for \Delta t} \times (F_{CH_4} \times \Delta t) \times (M_O / m_{ox}) ] \quad (18)$$

It can also be of interest to look at the overall conversion of CH<sub>4</sub>,  $\gamma_{CH_4}$ , see expression (19), and the specific conversion of CH<sub>4</sub> to CO<sub>2</sub>,  $\gamma_{red}$ , see expression (20).

$$\gamma_{CH_4} = [ x_{CO_2} + x_{CO} + c ] / [ x_{CH_4} + x_{CO_2} + x_{CO} + c ] \quad (19)$$

$$\gamma_{red} = [ x_{CO_2} ] / [ x_{CH_4} + x_{CO_2} + x_{CO} + c ] \quad (20)$$

The difference between chemical-looping combustion and chemical-looping reforming can be illustrated by defining a number  $\Psi$ , see expression (21).

$$\Psi = [ (2 \times x_{CO_2} + x_{H_2O} + x_{CO}) / (x_{CO_2} + x_{CO}) ] / 4 \quad (21)$$

$\Psi$  can be said to describe the degree of oxidation of gaseous products, excluding unreformed CH<sub>4</sub>. When  $\Psi$  is 1, this means that there is no CO and H<sub>2</sub> present, only CO<sub>2</sub>, H<sub>2</sub>O and CH<sub>4</sub>. When  $\Psi$  is 0.25, there is only CO, H<sub>2</sub> and CH<sub>4</sub> present and no CO<sub>2</sub> or H<sub>2</sub>O. For the numbers in between there is a mix of both reactions.  $\Psi_{min}$  is defined as the lowest  $\Psi$  achieved until carbon formation is believed to start, which is when calculated  $c/c_{tot}$  exceeds 4%.

For chemical-looping combustion  $\Psi$  and  $\gamma_{red}$  should be close to 1. For chemical-looping reforming focused on H<sub>2</sub> production,  $\Psi$  should be in the order of 0.30-0.35, see Rydén et al. (2006a, 2006b). For cogeneration of H<sub>2</sub>/CO and heat/power,  $\Psi$  could be anywhere between 0.35 and 1. These numbers for  $\Psi$  are based on the assumption that  $\gamma_{CH_4}$  can be almost 100% for practical applications. In this paper, a  $\Delta\omega$  interval where  $\Psi$  is 0.98 or higher is called  $\Delta\omega_{98}$ . If the conversion of CH<sub>4</sub> is high in this interval the tested oxygen-carrier could be suitable for chemical-looping combustion applications. In similar fashion, an interval where  $\Psi$  is 0.5 or lower and  $c/c_{tot}$  is below 4% is called  $\Delta\omega_{50}$ , and an interval where  $\Psi$  is 0.35 or lower and  $c/c_{tot}$  is below 4% is called  $\Delta\omega_{35}$ . If the conversion of CH<sub>4</sub> is high in those intervals the tested oxygen-carrier should be feasible for chemical-looping reforming applications. For some of the examined materials, there was an initial period of combustion, which was followed by a period of reforming. In a real-world reformer it should be possible to avoid the combustion period by not completely reoxidize the oxygen carrier in the air reactor, as was done for example in the experimental study by Rydén et al. (2006a).

In section 4.1-4.4 below the different oxygen carriers are compared to each other by plotting  $\gamma_{CH_4}$  as a function of  $\Psi$ . This gives a general idea of the potential of each material. High  $\gamma_{CH_4}$  is wanted, but materials with lower  $\gamma_{CH_4}$  should not necessarily be ruled out since it may be possible to improve  $\gamma_{CH_4}$  for practical applications, for example by increasing the bed height in the fuel reactor. Additionally, numerical values for  $\Delta\omega_{98}$ ,  $\Delta\omega_{50}$  and  $\Delta\omega_{35}$  have been estimated for relevant test cycles. These numbers gives an indication of how large share of an oxygen carrier that can be utilized for chemical-looping combustion and chemical-looping reforming respectively. Low values indicate that high circulation rate is needed between the air reactor and the fuel reactor and vice versa.  $\gamma_{red}$  has also been plotted as function of  $\Delta\omega$  which gives an idea of how well suited the material is for chemical-looping combustion specifically. Presented values for  $\Delta\omega$  shall be seen as somewhat rough estimations since they

depend heavily on oxygen released during the initial combustion period where there are large concentration gradients and measurements imperfections due to factors described above.

## 4. Results

### 4.1 $\text{La}_x\text{Sr}_{1-x}\text{Fe}_y\text{Co}_{1-y}\text{O}_{3-\delta}$ Perovskites

$\text{La}_{0.5}\text{Sr}_{0.5}\text{Fe}_{0.5}\text{Co}_{0.5}\text{O}_{3-\delta}$  was found to have properties that make it potentially well suited for chemical-looping combustion applications. There was high conversion of  $\text{CH}_4$  into  $\text{H}_2\text{O}$  and  $\text{CO}_2$  in the beginning of each reduction period. When  $\Delta\omega$  was in the order of 2%, the conversion of  $\text{CH}_4$  decreased rapidly and the reduction produced  $\text{H}_2\text{O}$ ,  $\text{CO}_2$  and minor amounts of  $\text{H}_2$  and  $\text{CO}$ . When  $\Delta\omega$  reached about 6%,  $\text{CH}_4$  started to decompose into  $\text{H}_2$  and solid carbon. For an example of a reduction curve, see Figure 3.

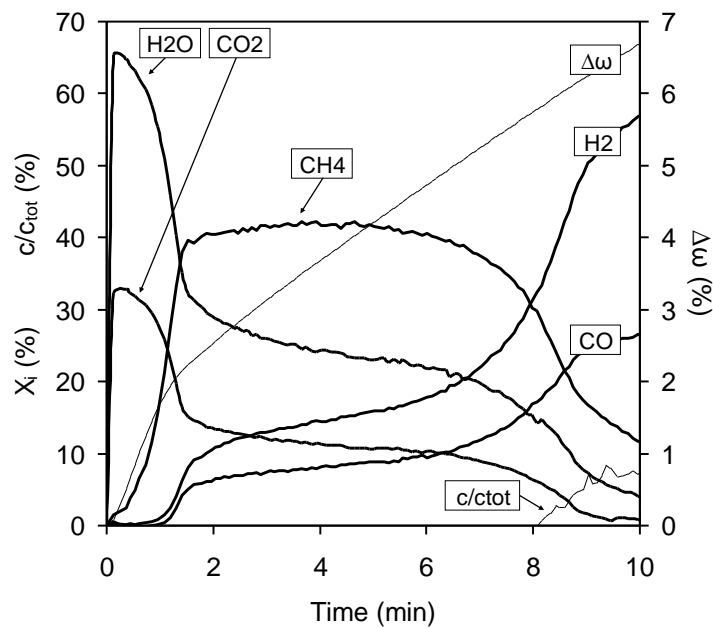


Figure 3. Reduction of  $\text{La}_{0.5}\text{Sr}_{0.5}\text{Fe}_{0.5}\text{Co}_{0.5}\text{O}_{3-\delta}$  with 9 ml/min  $\text{CH}_4$ , second cycle.

$\text{La}_{0.5}\text{Sr}_{0.5}\text{Fe}_{0.5}\text{Co}_{0.5}\text{O}_{3-\delta}$  responded well to increased  $\text{CH}_4$  flow. The conversion of  $\text{CH}_4$  remained high and  $d\omega_{98}/dt$  was found to be approximately proportional to the  $\text{CH}_4$  flow for flows up to 21 ml/min. This is not surprising since the reaction rate should be correlated to the reactant concentration. For even higher flows the conversion of  $\text{CH}_4$  decreased slightly. The tenth reduction cycle was about as good as the two first. Following the experiments, the sample was examined with XRD and it was found that it had maintained its perovskite structure. Performance data can be found in Table 5.

Sample	Material	Cycle (nr)	$F_{\text{CH}_4}$ (ml/min)	$\Delta\omega_{98}$ (%)	$d\omega_{98}/dt$ (%/min)
1	$\text{La}_{0.5}\text{Sr}_{0.5}\text{Fe}_{0.5}\text{Co}_{0.5}\text{O}_{3-\delta}$	1	9	1.7	1.7
1	$\text{La}_{0.5}\text{Sr}_{0.5}\text{Fe}_{0.5}\text{Co}_{0.5}\text{O}_{3-\delta}$	2	9	1.8	1.7
1	$\text{La}_{0.5}\text{Sr}_{0.5}\text{Fe}_{0.5}\text{Co}_{0.5}\text{O}_{3-\delta}$	3	15	1.8	2.5
1	$\text{La}_{0.5}\text{Sr}_{0.5}\text{Fe}_{0.5}\text{Co}_{0.5}\text{O}_{3-\delta}$	4	15	2.0	2.6
1	$\text{La}_{0.5}\text{Sr}_{0.5}\text{Fe}_{0.5}\text{Co}_{0.5}\text{O}_{3-\delta}$	10	9	2.0	1.8

Table 5. Performance for a few test cycles with  $\text{La}_{0.5}\text{Sr}_{0.5}\text{Fe}_{0.5}\text{Co}_{0.5}\text{O}_{3-\delta}$  perovskite.

For the perovskites that did not contain Co, the reduction could also be divided into three distinct periods. First there was a combustion period, where parts of the  $\text{CH}_4$  were oxidized to  $\text{H}_2\text{O}$  and  $\text{CO}_2$ . For  $\text{LaFeO}_{3-\delta}$  this period was very short, while it was more pronounced for  $\text{La}_{0.8}\text{Sr}_{0.2}\text{FeO}_{3-\delta}$ , and even more so for  $\text{La}_{0.5}\text{Sr}_{0.5}\text{FeO}_{3-\delta}$ . Following this was a period of partial oxidation where  $\text{CH}_4$  was converted mostly into  $\text{CO}$  and  $\text{H}_2$ . The  $\text{CH}_4$  conversion improved slightly as more  $\text{O}_2$  was drained from the sample. Finally,  $\text{CH}_4$  started to decompose to  $\text{H}_2$  and solid carbon. An example of a reduction curve for  $\text{La}_{0.8}\text{Sr}_{0.2}\text{FeO}_{3-\delta}$  can be found in Figure 4.

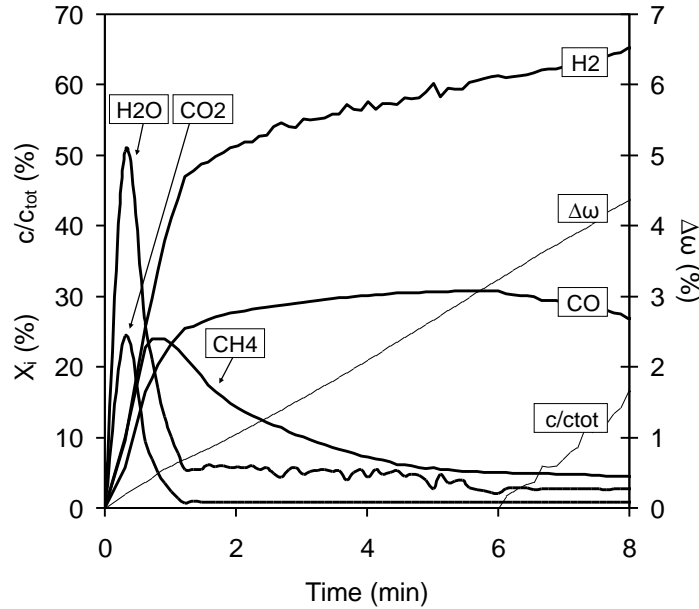


Figure 4. Reduction of  $\text{La}_{0.8}\text{Sr}_{0.2}\text{FeO}_{3-\delta}$  with 9 ml/min  $\text{CH}_4$ , second cycle.

In Figure 5,  $\gamma_{\text{CH}_4}$  has been plotted as a function of  $\Psi$ , and in Figure 6,  $\gamma_{\text{red}}$  has been plotted as a function of  $\Delta\omega$ , for the examined perovskites.

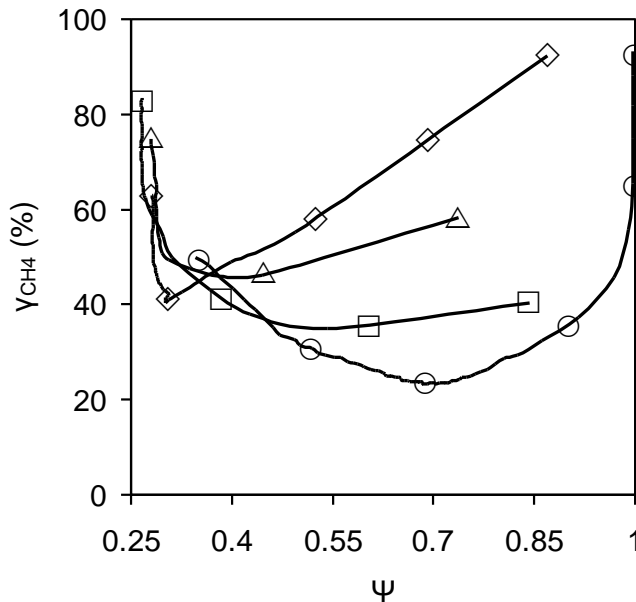


Figure 5.  $\gamma_{\text{CH}_4}$  as a function of  $\Psi$  for examined perovskites. Only periods where no carbon was formed have been included. The data is for the third reduction cycle and the symbols correspond to: ( $\circ$ )  $\text{La}_{0.5}\text{Sr}_{0.5}\text{Fe}_{0.5}\text{Co}_{0.5}\text{O}_{3-\delta}$ , ( $\square$ )  $\text{LaFeO}_{3-\delta}$ , ( $\triangle$ )  $\text{La}_{0.8}\text{Sr}_{0.2}\text{FeO}_{3-\delta}$ , ( $\diamond$ )  $\text{La}_{0.5}\text{Sr}_{0.5}\text{FeO}_{3-\delta}$ .

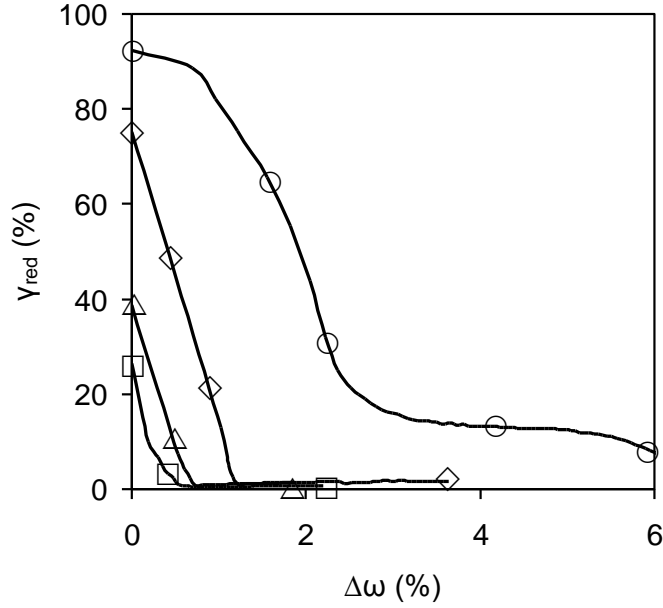


Figure 6.  $\gamma_{red}$  as a function of  $\Delta\omega$  for examined perovskites. Only periods where no carbon was formed have been included. The data is for the third reduction cycle and the symbols correspond to: (○)  $La_{0.5}Sr_{0.5}Fe_{0.5}Co_{0.5}O_{3-\delta}$ , (□)  $LaFeO_{3-\delta}$ , (△)  $La_{0.8}Sr_{0.2}FeO_{3-\delta}$ , (◇)  $La_{0.5}Sr_{0.5}FeO_{3-\delta}$ .

In Figure 5 and Figure 6 it can be seen that unlike  $La_{0.5}Sr_{0.5}Fe_{0.5}Co_{0.5}O_{3-\delta}$ , none of the  $La_xSr_{1-x}FeO_{3-\delta}$  perovskites provide high selectivity towards  $CO_2$  and  $H_2O$ . What makes these materials interesting is the second period of the reduction where partial oxidation of the fuel with very high selectivity towards  $H_2$  and  $CO$  occurred. In Figure 5 it can be seen that all examined  $La_xSr_{1-x}FeO_{3-\delta}$  perovskites reached  $\Psi$  well below 0.35 with high conversion of  $CH_4$  and with no carbon formation, so these materials can be interesting for chemical-looping reforming applications. Illustrative data related to chemical-looping reforming for a few test cycles of  $La_xSr_{1-x}FeO_{3-\delta}$  perovskite can be found in Table 6.

Sample	Material	Cycle (nr)	$F_{CH_4}$ (ml/min)	$\Psi_{min}$	$\Delta\omega_{35}$ (%)	$D\omega_{35}/dt$ (%/min)
2	$LaFeO_{3-\delta}$	1	9	0.26	2.3	0.4
2	$LaFeO_{3-\delta}$	2	9	0.27	1.6	0.5
2	$LaFeO_{3-\delta}$	3	15	0.27	1.8	0.8
2	$LaFeO_{3-\delta}$	4	15	0.27	1.5	0.7
2	$LaFeO_{3-\delta}$	10	9	-	-	-
3	$La_{0.8}Sr_{0.2}FeO_{3-\delta}$	1	9	0.28	3.2	0.6
3	$La_{0.8}Sr_{0.2}FeO_{3-\delta}$	2	9	0.28	2.9	0.5
3	$La_{0.8}Sr_{0.2}FeO_{3-\delta}$	3	15	0.28	0.9	0.6
3	$La_{0.8}Sr_{0.2}FeO_{3-\delta}$	4	15	0.28	1.0	0.6
3	$La_{0.8}Sr_{0.2}FeO_{3-\delta}$	10	9	0.28	1.3	0.5
4	$La_{0.5}Sr_{0.5}FeO_{3-\delta}$	1	9	0.31	3.1	0.4
4	$La_{0.5}Sr_{0.5}FeO_{3-\delta}$	2	9	0.32	2.4	0.5
4	$La_{0.5}Sr_{0.5}FeO_{3-\delta}$	3	15	0.28	2.5	0.5
4	$La_{0.5}Sr_{0.5}FeO_{3-\delta}$	4	15	0.28	2.5	0.5
4	$La_{0.5}Sr_{0.5}FeO_{3-\delta}$	10	9	0.29	2.4	0.4

Table 6. Chemical-looping reforming performance for a few test cycles with  $La_xSr_{1-x}FeO_{3-\delta}$  perovskite.

In Table 6 and Figure 5, it can be seen that  $\text{LaFeO}_{3-\delta}$  provided very low  $\Psi$  numbers.  $\Delta\omega_{35}$  was reduced somewhat after the first cycle, to about 1.5-1.8%.  $\text{LaFeO}_{3-\delta}$  could handle an increase in the  $\text{CH}_4$  flow to 15 ml/min without major changes in the  $\text{CH}_4$  conversion, the product composition or  $\Delta\omega_{35}$ . But eventually the properties of the sample changed so that carbon formation started more or less immediately. This happened when  $\text{CH}_4$  flows over 21 ml/min were used and the pattern remained when the gas flow was restored to the initial 9 ml/min. Somehow the material had been affected by the redox cycles and lost its favourable properties.

$\text{La}_{0.8}\text{Sr}_{0.2}\text{FeO}_{3-\delta}$  initially provided high conversion of  $\text{CH}_4$  and high selectivity towards CO and  $\text{H}_2$ . This material did not response well to increased  $\text{CH}_4$  flows though. With a  $\text{CH}_4$  flow of 15 ml/min  $\Delta\omega_{35}$  was reduced from about 3% to about 1%, and the conversion of  $\text{CH}_4$  decreased substantially.  $\text{La}_{0.8}\text{Sr}_{0.2}\text{FeO}_{3-\delta}$  also suffered from reduced performance in the tenth cycle, when the  $\text{CH}_4$  flow was restored to 9 ml/min. But unlike  $\text{LaFeO}_{3-\delta}$  it maintained at least some of its ability to convert  $\text{CH}_4$  to CO and  $\text{H}_2$  without carbon formation.

$\text{La}_{0.5}\text{Sr}_{0.5}\text{FeO}_{3-\delta}$  showed lower reactivity with  $\text{CH}_4$  and slightly lower selectivity towards CO and  $\text{H}_2$  than the other  $\text{La}_x\text{Sr}_{1-x}\text{FeO}_{3-\delta}$  perovskites.  $\Delta\omega_{35}$  was reduced slightly following the first reduction cycle, to about 2.5%. Then the particles seem to have maintained its properties well. The tenth and final reduction cycle was about as good as the early ones.

Loss in performance after reduction for  $\text{La}_x\text{Sr}_{1-x}\text{FeO}_{3-\delta}$  perovskites has been observed by Bjørgum (2005), who concluded that this could be due to permanent deactivation of the material by solid carbon. The results presented here suggest some other mechanism. For  $\text{La}_{0.8}\text{Sr}_{0.2}\text{FeO}_{3-\delta}$  and  $\text{LaFeO}_{3-\delta}$  carbon formation was recorded in the end of the first reduction cycles, but this did not seem to result in radical reduction of the material performance. The materials were altered slightly, but that was the case also for  $\text{La}_{0.5}\text{Sr}_{0.5}\text{FeO}_{3-\delta}$  where there was no carbon formation during the first reduction cycles. After the experiments the used samples were examined with XRD, and it could be concluded that all materials had maintained a perovskite structure and that there was no sign of decomposition into metals or metal oxides. So this should not have been a reason for the altered performance.

One possible explanation to the loss in performance is agglomeration. The perovskite particles stuck to each other and formed a flake following reduction and oxidation. This could be observed when the particle sample was to be removed. When the reactor was turned upside-down the perovskites did not just fall out of the reactor, but some mechanical force was necessary. Typically the majority of the particles in the used sample were found in a flake of agglomerated particles. The flake was quite hard and did not break up when shaken in a glass jar, but it could easily be pierced with a spoon. The agglomeration could have resulted in reduced effective surface area of the particles, and perhaps in formation of channels through the sample bed that could reduce the amount of active oxygen-carrier material.

To summarize the results, it was shown that reduction of  $\text{La}_x\text{Sr}_{1-x}\text{FeO}_{3-\delta}$  perovskites can provide very high selectivity towards CO and  $\text{H}_2$  without formation of solid carbon. All tested materials could produce gas with  $\Psi$  lower than 0.30, which should be appropriate for most chemical-looping reforming applications. It was also shown that  $\Delta\omega_{35}$  could be in the order of 1.5-3%. By contrast,  $\text{La}_{0.5}\text{Sr}_{0.5}\text{Fe}_{0.5}\text{Co}_{0.5}\text{O}_{3-\delta}$  had properties that make it feasible for chemical-looping combustion applications. It can be concluded that  $\text{La}_x\text{Sr}_{1-x}\text{Fe}_y\text{Co}_{1-y}\text{O}_{3-\delta}$  perovskites provide many interesting options to produce oxygen-carrier materials.

## 4.2 NiO/MgAl<sub>2</sub>O<sub>4</sub>

$\text{NiO/MgAl}_2\text{O}_4$  was found to be very reactive with  $\text{CH}_4$ . Measured  $\text{CH}_4$  concentrations in the outlet from the reactor were always close to zero. See Figure 7 for an example of a reduction curve.

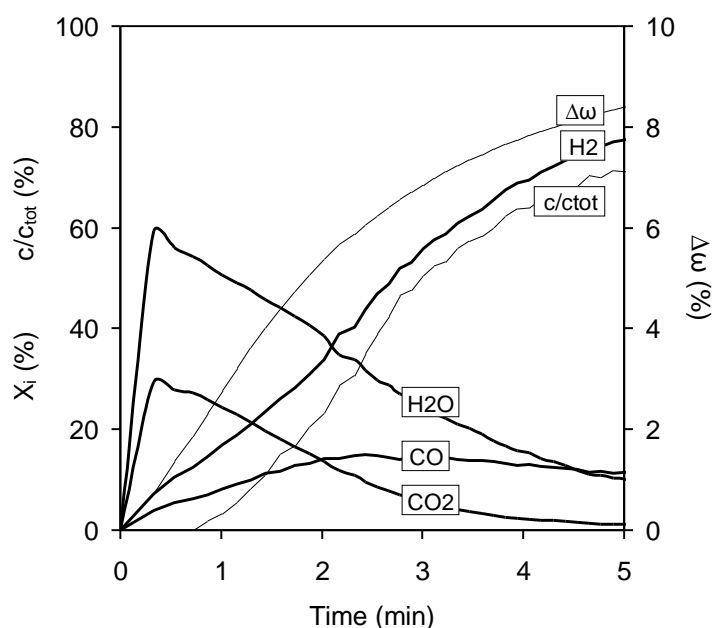


Figure 7. Reduction of 1.00 g NiO/MgAl<sub>2</sub>O<sub>4</sub> with 15 ml/min CH<sub>4</sub>, third cycle.

When NiO is reduced, metallic Ni is obtained, see reaction (22).



It is well known that metallic Ni catalyzes decomposition of CH<sub>4</sub> into H<sub>2</sub> and solid carbon, reaction (5). In Figure 7 it can be seen that this effect becomes apparent when  $\Delta\omega$  reaches about 2%, and from this point the formation of solid carbon increases rapidly.

$\Psi$  was never above 0.98, since small amounts of H<sub>2</sub> and CO were detected immediately in the first measured point in each reduction cycle. From a thermodynamical point of view, NiO lacks the ability to convert CH<sub>4</sub> completely to CO<sub>2</sub> and H<sub>2</sub>O. The equilibrium concentrations at 900°C are low, about 1.2% for H<sub>2</sub> and 0.8% for CO, but measured concentrations were higher. The tested NiO/MgAl<sub>2</sub>O<sub>4</sub>-particles were from a batch that previously has been used successfully for experiments in a continuously operating chemical-looping reactor with interconnected circulating fluidized beds, in which Johansson, E. et al. (2005, 2006a, 2006b) examined chemical-looping combustion at 800-950°C and Rydén et al. (2006a, 2006b) examined chemical-looping reforming at 820-930°C. The particles have also been examined with pulse experiments in a fluidized-bed reactor by Johansson, M. et al (2007). The experience from these studies is that the CO concentration does not reach values above 1-3% until a substantial share of the oxygen available on the particles has been removed.

One reason for the high concentrations of H<sub>2</sub> and CO provided by the experiments presented here could be that the oxygen-carrier properties may be dependent upon the temperature of reduction. In a study by Mattisson et al. (2006), it has been shown that the reactivity of NiO/MgAl<sub>2</sub>O<sub>4</sub> with CO and H<sub>2</sub> decreases at temperatures below 950°C. In the study presented here a reactor temperature of 900°C was used. Hence somewhat limited reactivity with CO and H<sub>2</sub> can be expected, while the reactivity with CH<sub>4</sub> remains very high due to the catalytic effect of metallic Ni.

It shall also be pointed out that when CH<sub>4</sub> is added from the top of a fixed-bed reactor, NiO on the bed surface will almost immediately be reduced to metallic Ni and thus create a catalytic surface that decomposes CH<sub>4</sub> and possibly also propagates carbon formation. This

should be compared with the conditions in a fluidized bed, where there is no static bed surface. Other possible explanation for the high concentrations of H<sub>2</sub> and CO includes agglomerations, sintering of particles, formation of channels in the sample bed etc. Just as the perovskite particles, the NiO/MgAl<sub>2</sub>O<sub>4</sub>-particles agglomerated into a solid flake as described in section 4.1 above.

At no occasion did  $\Psi$  reach values below 0.5 without substantial formation of solid carbon. This could possibly be addressed by adding some H<sub>2</sub>O to the CH<sub>4</sub>, which is a well known method to hamper formation of solid carbon on metal surfaces. The study by Rydén et al. (2006a) indicated that continuously operating chemical-looping reforming using NiO/MgAl<sub>2</sub>O<sub>4</sub> particles as oxygen carrier is possible and that 25 vol% H<sub>2</sub>O added to natural gas was sufficient to reduce carbon formation to very low numbers.

Data for the reduction cycles of NiO/MgAl<sub>2</sub>O<sub>4</sub>-particles can be found in section 4.3 below.

### 4.3 Fe<sub>2</sub>O<sub>3</sub>/MgAl<sub>2</sub>O<sub>4</sub> with NiO/MgAl<sub>2</sub>O<sub>4</sub>

Three different oxygen-carrier samples based on Fe<sub>2</sub>O<sub>3</sub>/MgAl<sub>2</sub>O<sub>4</sub> were evaluated, pure Fe<sub>2</sub>O<sub>3</sub>/MgAl<sub>2</sub>O<sub>4</sub> and the same material with 1% and 10% NiO/MgAl<sub>2</sub>O<sub>4</sub> respectively. The NiO is reduced according to reaction (22), while the reduction of Fe<sub>2</sub>O<sub>3</sub> takes place in 3 steps, see reactions (23-25).



For chemical-looping combustion applications, only reaction (23) is of interest. This is because there are thermodynamical constraints that limit the conversion of CH<sub>4</sub> to CO<sub>2</sub> and H<sub>2</sub>O for reactions (24-25). However, these reduction steps may still be useful for chemical-looping reforming applications.

In reaction (23-25), it can be seen that the amount of released oxygen increases for each reduction step. The oxygen carrier that was used in this study contained 40 mass% Fe<sub>2</sub>O<sub>3</sub>, and it can be calculated that reaction (23) should occur until  $\Delta\omega$  is about 1.3% and reaction (24) should occur until  $\Delta\omega$  is about 4.0%. Adding some NiO increases these numbers slightly, due to the high oxygen content of this metal oxide. In total,  $\Delta\omega$  should be limited to about 12.0%.

Fe<sub>2</sub>O<sub>3</sub>/MgAl<sub>2</sub>O<sub>4</sub> with or without added NiO/MgAl<sub>2</sub>O<sub>4</sub> was found to have properties that make it interesting both for chemical-looping combustion and chemical-looping reforming. See Figure 8 for an example of a reduction curve, which describes a principal appearance of the other reduction curves as well.

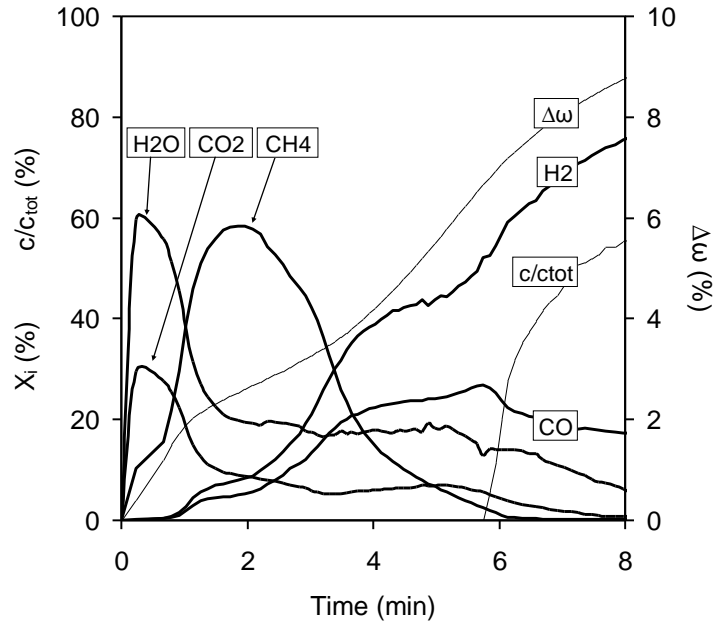


Figure 8. Reduction of 0.99 g  $Fe_2O_3/MgAl_2O_4$  and 0.01 g  $NiO/MgAl_2O_4$  with 15 ml/min  $CH_4$ , first cycle.

Since the reduction of  $Fe_2O_3$  involves several steps, it is not surprising that  $Fe_2O_3$ -based oxygen carriers could prove to be useful both for chemical-looping combustion and chemical-looping reforming applications. This versatility is illustrated in Figure 9, where  $\gamma_{CH_4}$  has been plotted as a function of  $\Psi$  and  $\Delta\omega$ . In Figure 10  $\gamma_{red}$  has been plotted as a function of  $\Delta\omega$ . Data for the  $NiO/MgAl_2O_4$  oxygen carrier have also been included.

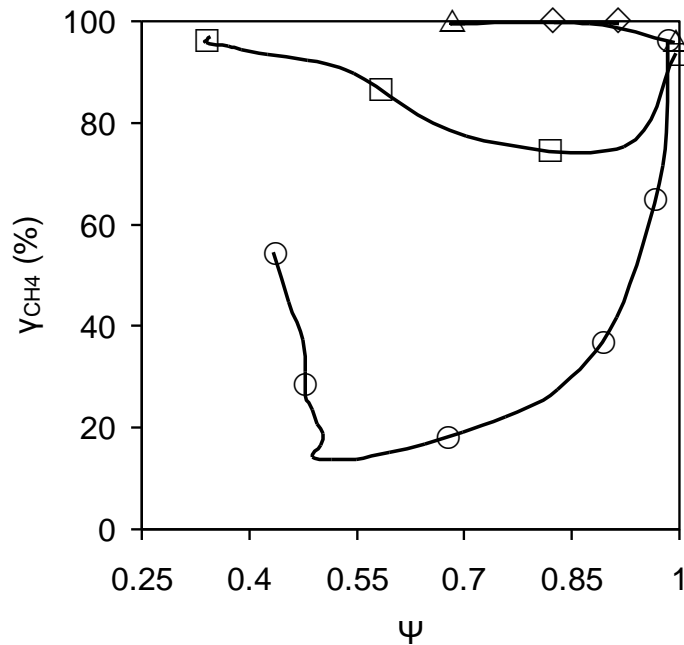


Figure 9.  $\gamma_{CH_4}$  as a function of  $\Psi$  for some different metal-oxide samples. Only periods where no carbon was formed have been included. The data is for the third reduction cycle and the symbols correspond to: (○) Fe100, (□) Fe99Ni1, (△) Fe90Ni10, (◇) Ni100.

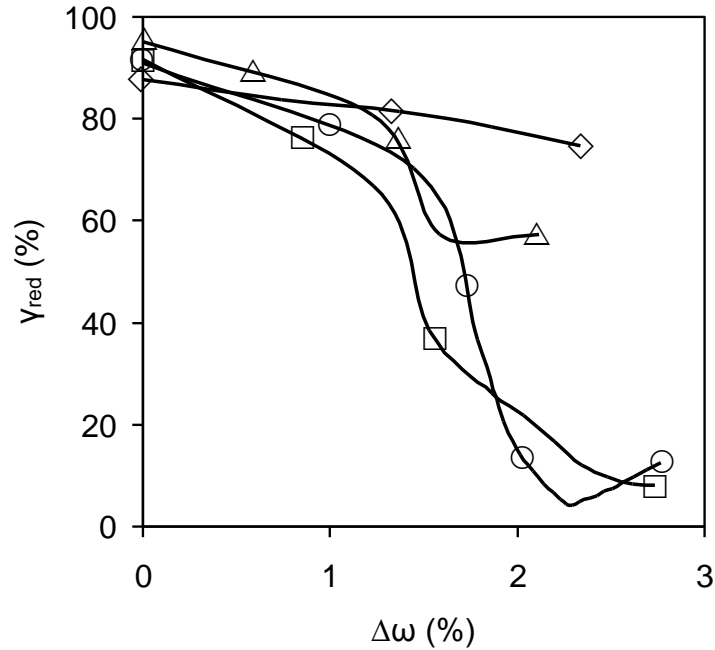


Figure 10.  $\gamma_{red}$  as a function of  $\Delta\omega$  for some different metal-oxide samples. Only periods where no carbon was formed have been included. The data is for the third reduction cycle and the symbols correspond to: (○) Fe100, (□) Fe99Ni1, (△) Fe90Ni10, (◇) Ni100.

In Figure 9, it can be seen that adding Ni to the sample increases the overall reactivity with  $\text{CH}_4$  greatly. It can also be seen that the sample containing 10% NiO/ $\text{MgAl}_2\text{O}_4$  had properties somewhat resembling those of 100% NiO/ $\text{MgAl}_2\text{O}_4$ .

For the samples with no or 1% NiO, there was a short combustion period when  $\text{CH}_4$  was converted into  $\text{CO}_2$  and  $\text{H}_2\text{O}$ . According to the estimations this period lasted until  $\Delta\omega$  was in the order of 1.1-1.5%. These numbers are based on very few measuring points, and as is explained in section 3.4, there are measurement imperfections in the beginning of each reduction cycle due to transients. But it seems reasonable to believe that this initial combustion period corresponds to reaction (23) which, according to the thermodynamics, should produce only  $\text{CO}_2$  and  $\text{H}_2\text{O}$  and should proceed until  $\Delta\omega$  reaches about 1.3%. In Figure 10, it can be seen that adding Ni to the sample did not prevent rapidly reduced  $\gamma_{red}$  once  $\Delta\omega$  values above 1.3% was obtained.

Following the combustion period was a period with reduced conversion of  $\text{CH}_4$ . Eventually the reactivity improved and the selectivity towards  $\text{H}_2$  and CO increased, and for a period there was partial oxidation of the fuel with decent selectivity towards CO and  $\text{H}_2$ . Finally,  $\text{CH}_4$  started to decompose into  $\text{H}_2$  and solid carbon. A summary of numerical data for the experiments can be found in Table 7, in which data for both  $\Delta\omega_{98}$  and  $\Delta\omega_{50}$  have been included.

Sample	Material	Cycle (nr)	$F_{CH_4}$ (ml/min)	$\Delta\omega_{98}$ (%)	$d\omega_{98}/dt$ (%/min)	$\Psi_{min}$	$\Delta\omega_{50}$ (%)	$d\omega_{50}/dt$ (%/min)
5	Ni100	1	15	-	-	0.59	-	-
5	Ni100	2	15	-	-	0.83	-	-
5	Ni100	3	15	-	-	0.83	-	-
6	Fe100	1	15	1.4	1.8	0.51	-	-
6	Fe100	2	15	1.3	2.0	0.43	0.7	0.5
6	Fe100	3	15	1.5	2.1	0.43	0.5	0.5
8	Fe99Ni1	1	15	1.5	1.9	0.39	3.2	1.3
8	Fe99Ni1	2	15	1.1	2.0	0.35	0.9	1.5
8	Fe99Ni1	3	15	1.2	1.9	0.34	0.7	1.5
9	Fe90Ni10	1	15	1.3	1.7	0.63	-	-
9	Fe90Ni10	2	15	1.2	2.4	0.63	-	-
9	Fe90Ni10	3	15	1.2	2.5	0.68	-	-

Table 7. Performance for a few test cycles with  $Fe_2O_3/MgAl_2O_4$  and  $NiO/MgAl_2O_4$ .

In table 7, it can be seen that all samples changed properties following the first reduction cycle. For chemical-looping combustion  $d\omega_{98}/dt$  increased somewhat. This behaviour is documented from tests of similar particles in fluidized beds. For chemical-looping reforming  $\Psi_{min}$  and  $\Delta\omega_{50}$  decreased. Those changes are likely an effect of changes in the surface and pore structure of the materials, following the first redox cycle. Unlike the perovskite particles and the  $NiO/MgAl_2O_4$  particles the iron based samples did not form any kind of hard agglomerations.

In Table 7 and Figure 9 it can be seen that adding 1%  $NiO/MgAl_2O_4$  improved the performance for the chemical-looping reforming period greatly. The  $CH_4$  conversion and  $d\omega_{50}/dt$  was improved and lower  $\Psi$  was allowed without carbon formation.  $\Psi$  values below 0.35 with  $\gamma_{CH_4}$  well over 90% were achieved. This should be sufficient for practical chemical-looping reforming applications and the numbers could probably be improved further by adding some  $H_2O$  to the fuel, which is known to hamper the formation of solid carbon.

Adding  $NiO$  to the sample did not result in any overwhelmingly positive effect for the initial chemical-looping combustion period.  $\gamma_{CH_4}$  is not improved and in Table 7 it can be seen that  $d\omega_{98}/dt$  did increase somewhat for the sample with 10%  $NiO$  though. This was due to improved conversion of  $CH_4$ , likely due to the catalytic effects of  $Ni$ .

#### 4.4 $Mn_3O_4/Mg-ZrO_2$ with $NiO/MgAl_2O_4$

Three different oxygen-carrier samples based on  $Mn_3O_4/Mg-ZrO_2$  were evaluated, pure  $Mn_3O_4/Mg-ZrO_2$  and the same material mixed with 3% and 10%  $NiO/MgAl_2O_4$  respectively.  $NiO$  is reduced according to reaction (22), while  $Mn_3O_4$  is reduced according to reaction (26).



Under the conditions used, further reduction to metallic  $Mn$  should not be possible from a thermodynamic point of view. While oxidation to  $Mn_2O_3$  in the air reactor is thermodynamically possible, this reaction is not believed to happen to any larger extent. For a particle that is made from of 40 mass%  $Mn_3O_4$ , this means that  $\Delta\omega$  is limited to about 3%. Adding  $NiO$  to the sample increases this number slightly.

All experiments performed with  $Mn_3O_4$ , with or without added  $NiO$ , produced similar results. In the beginning of each reduction period,  $CH_4$  was converted to  $CO_2$  and  $H_2O$ . When

$\Delta\omega$  was in the order of 2.5-3.0%, this reaction stopped abruptly. See Figure 11 for a reduction curve where Ni was present.

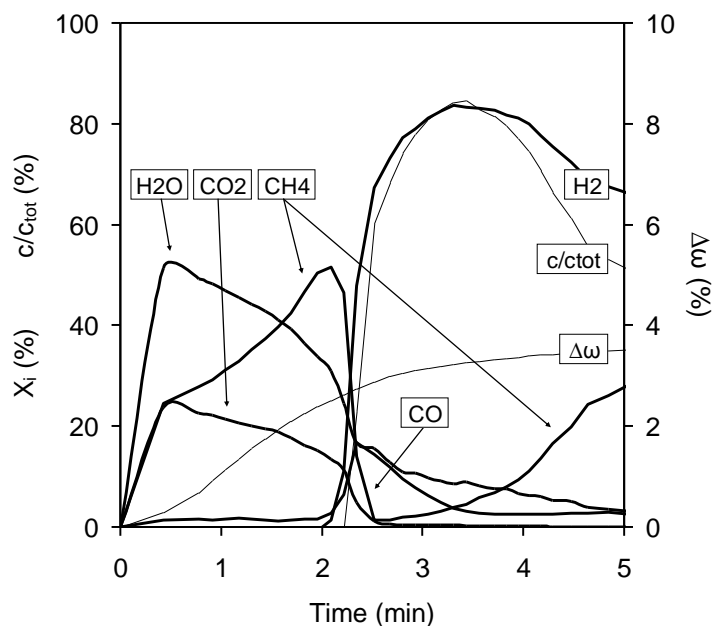


Figure 11. Reduction of 97%  $Mn_3O_4/Mg-ZrO_2$  and 3%  $NiO/MgAl_2O_4$  with 15 ml/min  $CH_4$ , first cycle.

In Figure 12,  $\gamma_{CH_4}$  has been plotted as a function of  $\Psi$ .

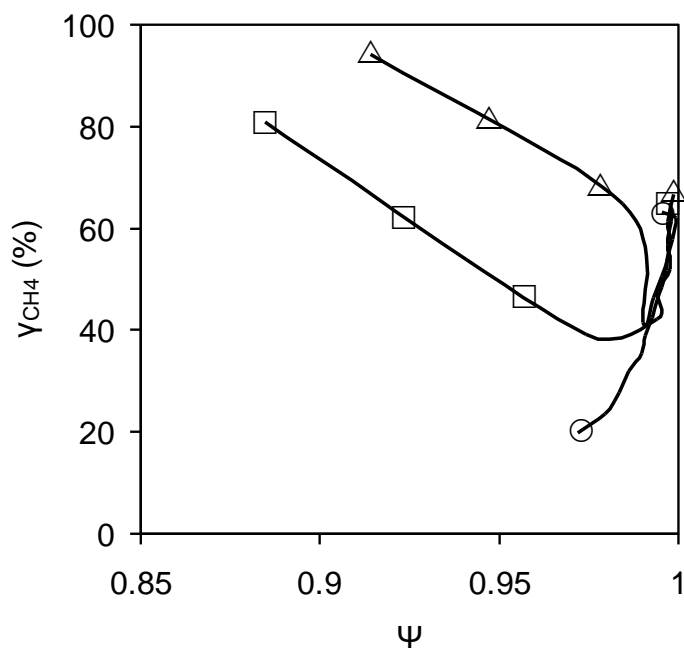


Figure 12.  $\gamma_{CH_4}$  as a function of  $\Psi$  for some metal-oxide samples. Only periods where no carbon was formed have been included. The data is for the third reduction cycle and the symbols correspond to: (○) Mn100, (□) Mn97Ni3, (△) Mn90Ni10.

In Figure 13,  $\gamma_{red}$  has been plotted as a function of  $\Delta\omega$ .

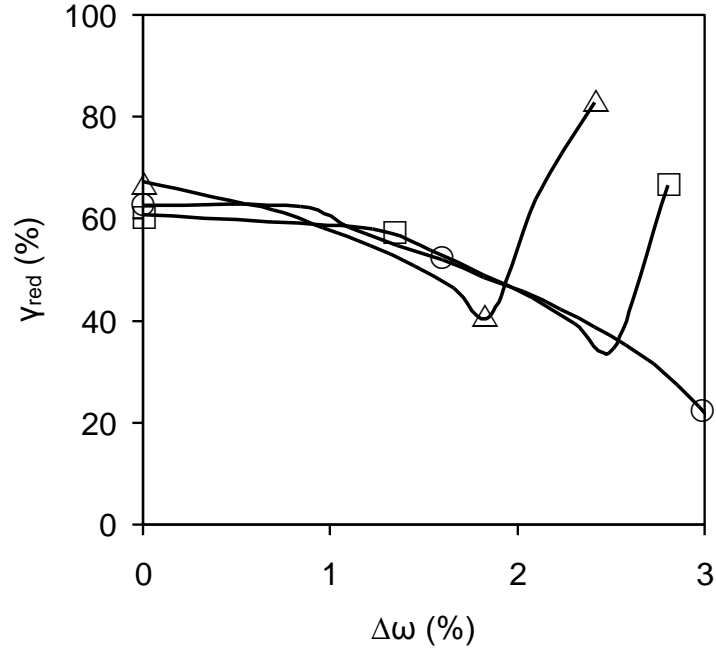


Figure 13.  $\gamma_{red}$  as a function of  $\Delta\omega$  for some metal-oxide samples. Only periods where no carbon was formed have been included. The data is for the third reduction cycle and the symbols correspond to: (○) Mn100, (□) Mn97Ni3, (△) Mn90Ni10.

The results indicate that oxygen carriers based on  $Mn_3O_4/Mg-ZrO_2$  are well suited for chemical-looping combustion applications. A summary of the performance for a few cycles can be found in Table 8.

Sample	Material	Cycle (nr)	$F_{CH_4}$ (ml/min)	$\Delta\omega_{98}$ (%)	$d\omega_{98}/dt$ (%/min)
8	Mn100	1	15	2.6	1.3
8	Mn100	2	15	2.9	1.8
8	Mn100	3	15	2.9	1.7
10	Mn97Ni3	1	15	2.4	1.2
10	Mn97Ni3	2	15	2.3	1.7
10	Mn97Ni3	3	15	2.5	1.7
11	Mn90Ni10	1	15	2.4	1.3
11	Mn90Ni10	2	15	2.4	1.8
11	Mn90Ni10	3	15	2.1	1.7

Table 8. Chemical-looping combustion performance for a few test cycles with  $Mn_3O_4/Mg-ZrO_2$  and  $NiO/MgAl_2O_4$ .

In Figure 12, it can be seen that all samples had about the same  $\gamma_{CH_4}$  when  $0.98 < \Psi$ . In Figure 13, it can be seen that all samples had about the same  $\gamma_{red}$  when  $1.8\% > \Delta\omega$ . Here the curves are so close together that they barely can be separated from each other. So for the period suitable for chemical-looping combustion, adding NiO to the sample did not appear to have had any positive effect. In Table 8 it can be seen that  $d\omega_{98}/dt$  was about the same for all samples, with exception that the reactivity increased considerably after the first reduction cycle, just as for the samples based on  $Fe_2O_3$ . No agglomerations were formed. One possible difference between the samples was that with 10% NiO added,  $\Delta\omega_{98}$  seemed to decrease slightly due to earlier carbon formation, as is illustrated in Figure 13.

In Figure 12 and Figure 13 it can also be seen that the chemical-looping combustion period was followed by rapidly improved  $\gamma_{CH_4}$  followed by carbon formation for the samples with NiO present, while the sample without NiO lost reactivity and soon most of the  $CH_4$  just passed right through the reactor without any reaction. At no occasion, were low  $\Psi$  and high  $\gamma_{CH_4}$  achieved without carbon formation.

In Tables (7-8) it can be seen that  $d\omega_{98}/dt$  for the particles of  $Mn_3O_4/Mg-ZrO_2$  is slightly lower than  $d\omega_{98}/dt$  for the particles of  $Fe_2O_3/MgAl_2O_4$ . In Figures (7-13) it can be seen that the initial conversion of  $CH_4$  is higher for the  $Fe_2O_3$ -based samples. This shall be compared to the numbers presented by Johansson et al. (2006b), who examined the redox properties of similar materials and found that the  $Mn_3O_4$ -based particles had about 30% better reactivity with  $CH_4$  than the  $Fe_2O_3$ -based particles. The reason for the differing results could be due to the different experimental conditions. Johansson et al. (2006b) defined a rate index based on the moment with the best reaction kinetics, here an average for the whole  $\Delta\omega_{98}$  interval was used. Other differences between the experiments is that Johansson et al. (2006b) used fluidized-bed reactor,  $CH_4$  mixed with 50 vol% steam as fuel for reduction, twice as high fuel to oxygen carrier load and a reactor temperature of 950°C.

## 5. Discussion

From the tests with the relatively well documented metal-oxide materials, it can be seen that there are some differences between testing oxygen-carrier particles in a fixed-bed reactor compared to using a fluidized-bed reactor. This was especially true for the NiO based samples. There are many possible reasons for this. One could be the static surface of the sample in a fixed-bed reactor, which has been discussed above. Other possible reasons include formation of channels or that large temperature gradients in the sample occurred.

One of the aims with the experiments presented here was to study if and when carbon formation occurs on different oxygen-carrier materials. Therefore no steam was added to the fuel, which could have been used to suppress formation of solid carbon. This should be borne in mind when comparing the results with those from other studies. Adding steam, or possibly  $CO_2$ , to the fuel could probably have been used to suppress carbon formation and thus improve the chemical-looping reforming performance, at least for NiO/ $MgAl_2O_4$  and  $Fe_2O_3/MgAl_2O_4$  with NiO/ $MgAl_2O_4$ , and possibly for perovskites as well.

The tested perovskite materials were plain particles of active material and nothing had been done to improve factors such as mechanical stability and surface area. In contrast, the tested metal oxides were supported on stable inert phases and had been selected after a few years of material screening in fluidized-bed reactors. This should be considered when comparing the results between the different oxygen carriers. The metal oxides are proven materials that can withstand hundreds of oxidation and reduction cycles in the harsh environment that is a fluidized bed, while the long-term chemical and mechanical properties of the perovskite particles are largely unknown. On the other hand, if some effort was put into the manufacturing process for this kind of perovskites, it may be possible to improve the properties of such materials significantly.

## 6. Conclusions

Several oxygen-carrier materials for chemical-looping applications have been tested by reduction with  $CH_4$  and oxidation with air in a fixed-bed reactor.

It was found that  $La_{0.5}Sr_{0.5}Fe_{0.5}Co_{0.5}O_{3-\delta}$  should be feasible for chemical-looping combustion applications.  $\Delta\omega_{98}$  was about 2% and  $d\omega_{98}/dt$  was in the same order as for the

tested materials based on  $\text{Fe}_2\text{O}_3$ .  $\text{La}_{0.5}\text{Sr}_{0.5}\text{Fe}_{0.5}\text{Co}_{0.5}\text{O}_{3-\delta}$  does not seem to provide any obvious advantages compared to proven metal-oxide materials though.

$\text{La}_x\text{Sr}_{1-x}\text{FeO}_{3-\delta}$  perovskites was found to be well suited for chemical-looping reforming applications.  $\Delta\omega_{35}$  could be 1.5-3.0 mass% or possibly higher. The selectivity towards CO and  $\text{H}_2$  was very high, with  $\Psi$  numbers of 0.30 or lower. Substituting La for Sr increased  $\Delta\omega_{35}$  but reduced the selectivity towards  $\text{H}_2$  and CO and the reactivity with  $\text{CH}_4$ .

$\text{NiO}/\text{MgAl}_2\text{O}_4$  propagated early formation of solid carbon, likely due to the catalytic properties of metallic Ni.

$\text{Fe}_2\text{O}_3/\text{MgAl}_2\text{O}_4$ , with or without added  $\text{NiO}/\text{MgAl}_2\text{O}_4$ , was found to have properties that could be useful both for chemical-looping combustion and chemical-looping reforming. Initially there was high conversion of  $\text{CH}_4$  into  $\text{CO}_2$  and  $\text{H}_2$ .  $\Delta\omega_{98}$  was in the order of 1.1-1.5% so this was most likely the reaction when  $\text{Fe}_2\text{O}_3$  was reduced to  $\text{Fe}_3\text{O}_4$ . For the chemical-looping combustion period, no positive effects could be verified by adding NiO to the sample. Later during the reduction there was a period with good selectivity towards CO and  $\text{H}_2$  that could be utilized for chemical-looping reforming. Here adding 1% NiO to the sample increased both reactivity and selectivity towards CO and  $\text{H}_2$  greatly.  $\Psi$  could be 0.35 or lower, and  $d\omega/dt$  was more than twice as high compared to the  $\text{La}_x\text{Sr}_{1-x}\text{FeO}_{3-\delta}$  perovskites.

$\text{Mn}_3\text{O}_4/\text{Mg-ZrO}_2$  with or without added  $\text{NiO}/\text{MgAl}_2\text{O}_4$  was found to be suitable only for chemical-looping combustion applications. At no occasions any significant formation of CO and  $\text{H}_2$  without carbon formation was observed. It could not be verified that adding NiO to the sample produced any positive effects.  $\Delta\omega_{98}$  was in the order of 2.4-2.9% and the reactivity with  $\text{CH}_4$  was slightly lower than for the  $\text{Fe}_2\text{O}_3$ -based materials.

## 7. Acknowledgements

The authors wish to thank our supporters and financiers, Nordisk Energiforskning via the Nordic  $\text{CO}_2$  Sequestration Program (No $\text{CO}_2$ ) and the Swedish Gas Centre (SGC).

## 8. References

- Abad, A., Mattisson, T., Lyngfelt, A., Rydén, M., 2006. Chemical-looping combustion in a 300 W continuously operating reactor system using a manganese-based oxygen carrier. *Fuel*, 85, 1174-1185.
- Abad, A., Mattisson, T., Lyngfelt, A., Johansson, M., 2007. The use of iron oxide as oxygen carrier in a chemical-looping reactor. *Fuel*, in press 2006. *Fuel*, 86, 1021-1035.
- Adánez, J., De Diego, L. F., García-Labiano, F., Gayán, P., Abad, A., 2003. Selection of oxygen carriers for chemical-looping combustion. *Energy & Fuels*, 18, 371-377.
- Adanez, J., Gayan, P., Celaya, J., De Diego, L., Garcia-Labiano, F., Abad, A., 2006. Behavior of a  $\text{CuO-Al}_2\text{O}_3$  oxygen carrier in a 10 kW chemical-looping combustion plant. *Proceedings of the 19th International Conference on Fluidized Bed Combustion*, Vienna, Austria.
- Bjørgum, E., 2005. Methane conversion over mixed metal oxides. Doctoral thesis, Norwegian University of Science and Technology, Trondheim, Norway.
- Blom, R., Readman, J. E., Olafsen, A., Larring, Y., 2005.  $\text{La}_{0.8}\text{Sr}_{0.2}\text{Fe}_{0.8}\text{Co}_{0.2}\text{O}_{3-\delta}$  as a potential oxygen carrier in chemical looping type reactor, an in-situ powder X-ray diffraction study. *Journal of Materials Chemistry*, 5, 1931-1937.
- Brandvoll, Ø., 2005. Chemical looping combustion: fuel conversion with inherent  $\text{CO}_2$  capture. Doctoral thesis, Norwegian University of Science and Technology, Trondheim, Norway.
- Cho, P., 2005. Development and characterization of oxygen-carrier materials for chemical-looping combustion. Doctoral thesis, Chalmers University of Technology, Göteborg, Sweden.

- Cho, P., Mattisson, T., Lyngfelt, A., 2005. Carbon formation on nickel and iron oxide-containing oxygen carriers for chemical-looping combustion. *Industrial & Engineering Chemistry Research*, 44, 668-676.
- Fathi, M., Bjørgum, E., Viig, T., Rokstad, O.A., 2000. Partial oxidation of methane to synthesis gas: Elimination of gas phase oxygen. *Catalysis Today*, 63, 489-497.
- Fossdal, A., 2007. Phase relations, thermal and mechanical properties of LaFeO<sub>3</sub>-based ceramics. Doctoral thesis, Norwegian University of Science and Technology, Trondheim, Norway.
- Gavalas, G.R., Kim, K., Pantu, O., 2000. Methane partial oxidation on Pt/CeO<sub>2</sub>-ZrO<sub>2</sub> in absence of gaseous oxygen. *Applied Catalysis A: General*, 193, 203-214.
- Jalibert, J.C., Fathi, M., Rokstad, O.A., Holmen, A., 2001. Synthesis gas production by partial oxidation of methane from the cyclic gas-solid reaction using promoted cerium oxide. *Studies in Surface Science and Catalysis*, 136, 301-306.
- Jerndal, E., Mattisson, T., Lyngfelt, A., 2006. Thermal Analysis of Chemical-Looping Combustion. *Chemical Engineering Research and Design*, 84, 795-806.
- Johansson, E., 2005. Fluidized-bed reactor systems for chemical-looping combustion with inherent CO<sub>2</sub> capture. Doctoral thesis, Chalmers University of Technology, Göteborg, Sweden.
- Johansson, E., Mattisson, T., Lyngfelt, A., Thunman, H., 2006a. Combustion of syngas and natural gas in a 300 W chemical-looping combustor. *Chemical Engineering Research and Design*, 84, 819-827.
- Johansson, E., Mattisson, T., Lyngfelt, A., Thunman, H., 2006b. A 300 W laboratory reactor system for chemical-looping combustion with particle circulation. *Fuel*, 85, 1428-1238.
- Johansson, M., 2005. Selection of oxygen carriers for chemical-looping combustion using methane as fuel. Licentiate thesis, Chalmers University of Technology, Göteborg, Sweden.
- Johansson, M., Mattisson, T., Lyngfelt, A., 2006a. Creating a synergy effect by using mixed oxides of iron- and nickel oxides in the combustion of methane in a chemical-looping combustion reactor. *Energy & Fuels*, 20, 2399-2407.
- Johansson, M., Mattisson, T., Lyngfelt, A., 2006b. Comparison of oxygen carriers for chemical-looping combustion. *Thermal Science*, 10, 93-107.
- Johansson, M., Mattisson, T., Lyngfelt, A., Abad, A., 2007. Using pulse experiments to compare two promising nickel oxides for use in chemical-looping technologies. Submitted for publication.
- Kronberger, B., 2005. Modelling analysis of fluidised bed reactor systems for chemical-looping combustion. Doctoral thesis, Vienna University of Technology, Vienna, Austria.
- Lea Lein, H., 2005. Mechanical properties and phase stability of oxygen permeable membranes La<sub>0.5</sub>Sr<sub>0.5</sub>Fe<sub>1-x</sub>Co<sub>x</sub>O<sub>3-δ</sub>. Doctoral thesis, Norwegian University of Science and Technology, Trondheim, Norway.
- Li, R., Yu, C., Zhu, G., Shen, S., 2005. Methane oxidation to synthesis gas using lattice oxygen in La<sub>1-x</sub>Sr<sub>x</sub>MO<sub>3-δ</sub> (M = Fe, Mn) perovskite oxides instead of molecular oxygen. *Petroleum Science*, 2, 19-23.
- Lyngfelt, A., Kronberger, B., Adánez, J., Morin, J.X., Hurst, P., 2004. The GRACE project. Development of oxygen carrier particles for chemical-looping combustion. Design and operation of a 10 kW chemical-looping combustor. Proceedings of the 7<sup>th</sup> International Conference on Greenhouse Gas Control Technologies, Vancouver, Canada.
- Mattisson, T., Zafar, Q., Lyngfelt, A., Gevert, B., 2004. Integrated hydrogen and power production from natural gas with CO<sub>2</sub> capture. Proceedings of the 15<sup>th</sup> World Hydrogen Energy Conference, Yokohama, Japan.

Mattisson, T., Johansson, M., Lyngfelt, A., 2006. CO<sub>2</sub> capture from coal combustion using chemical-looping combustion – reactivity investigation of Fe, Ni and Mn based oxygen carriers using syngas. Proceedings of the 8<sup>th</sup> International Conference on Greenhouse Gas Control Technologies, Trondheim, Norway.

Mattisson, T., Lyngfelt, A., 2001. Applications of chemical-looping combustion with capture of CO<sub>2</sub>. Proceedings of the 2<sup>th</sup> Nordic Minisymposium on Carbon Dioxide Capture and Storage, Göteborg, Sweden.

Naqvi, R., 2006. Analysis of gas-fired power cycles with chemical looping combustion for CO<sub>2</sub> capture. Doctoral thesis, Norwegian University of Science and Technology, Trondheim, Norway.

Rydén, M., Lyngfelt, A., Mattisson, T., 2006a. Synthesis gas generation by chemical-looping reforming in a continuously operating laboratory reactor. *Fuel*, 85, 1631-1641.

Rydén, M., 2006b. Hydrogen production with carbon dioxide capture by reforming of natural gas using chemical-looping technologies. Licentiate thesis, Chalmers University of Technology, Göteborg, Sweden.

Ryu, H.J., Jin, G.T., Yi, C.K., 2004. Demonstration of inherent CO<sub>2</sub> separation and no NO<sub>x</sub> emission in a 50 kW chemical-looping combustor - continuous reduction and oxidation experiment. Poster presented at the 7<sup>th</sup> International Conference on Greenhouse Gas Control Technologies, Vancouver, Canada.

Stobbe, E.R., De Boer, B.A., Geus, J.W., 1999. The reduction and oxidation behaviour of manganese oxides. *Catalysis Today*, 47, 161-167.

Shen, S., Yu, C., Li, R., 2002. Partial oxidation of methane to synthesis gas using lattice oxygen of La<sub>1-x</sub>Sr<sub>x</sub>FeO<sub>3</sub> perovskite oxide catalysts instead of molecular oxygen. *Journal of Natural Gas Chemistry*, 11, 137-144.

Shen, S.K., Yu, C.C., Li, R.J., Ji, W.J., 2004. Methane oxidation to synthesis gas using lattice oxygen in La<sub>1-x</sub>Sr<sub>x</sub>FeO<sub>3</sub> perovskite oxides instead of molecular oxygen. *Studies in Surface Science and Catalysis*, 147, 139-144.

Wolf, J., 2004. CO<sub>2</sub> mitigation in advanced power cycles. Doctoral thesis, the Royal Institute of Technology, Stockholm, Sweden.

Zafar, Q., Mattisson, T., Gevert, B., 2005. Integrated hydrogen and power production with CO<sub>2</sub> capture using chemical-looping reforming - redox reactivity of particles of CuO, Mn<sub>2</sub>O<sub>3</sub>, NiO, and Fe<sub>2</sub>O<sub>3</sub> using SiO<sub>2</sub> as a support. *Industrial & Engineering Chemistry Research*, 44, 3485-3498.

Zeng, Y., Tamhankar, S., Ramprasad, N., Fitch, F., Acharya, D., Wolf, R., 2003. A novel cyclic process for synthesis gas production. *Chemical Engineering Science*, 58, 577-582.